Partial depletion of sarcoplasmic reticulum calcium does not prevent calcium sparks in rat ventricular myocytes

Long-Sheng Song, Michael D. Stern*, Edward G. Lakatta and Heping Cheng*

Laboratory of Cardiovascular Science, Gerontology Research Centre, National Institute on Aging, National Institutes of Health, Baltimore, MD 21224, USA

1. The exact nature of calcium sparks in the heart remains highly controversial. We sought to determine whether calcium sparks arise from a single or multiple calcium release channels/ryanodine receptors in the sarcoplasmic reticulum (SR). If their genesis involves a calcium-coupled recruitment of multiple channels, calcium sparks might be abolished by a modest depletion of SR calcium (because of the decrease in unitary calcium flux and hence a decrease in the gain of local calcium-induced calcium release). If, on the other extreme, calcium sparks are produced despite severe SR depletion, the single-channel origin will be preferred.

2. Spontaneous calcium sparks were studied in rat ventricular myocytes using confocal microscopy and the fluorescent calcium probe fluo-3. A computer algorithm was developed to count and measure objectively calcium sparks in linescan images.

3. Thapsigargin (25–150 nM) depleted caffeine-releasable SR calcium by up to 64%, in a dose- and time-dependent manner, without altering the resting cytosolic calcium level. During SR depletion, calcium sparks were robustly observed, albeit at reduced frequency ($\geqslant$ 30% of control) and amplitude ($\geqslant$ 60% of control).

4. Due to the reduced detectability of small sparks against noise background, the observed data would overestimate reduction in spark frequency but underestimate amplitude reduction. After correction for this detection bias, we found that the spark frequency was independent of SR load, whereas the amplitude was proportional to load.

5. We conclude that, although spark amplitude depends on SR filling status, the frequency of spark generation is independent of SR calcium load, and therefore independent of the local calcium release rate. This implies that sparks are single-channel events, or collective events that are well above threshold for local regeneration. Additionally, our results suggest that intraluminal SR calcium, at normal or low loads, does *not* play a major role in the regulation of on-gating of the ryanodine receptor.

The contraction of cardiac muscle is activated by a rise in cytoplasmic calcium concentration, $[Ca^{2+}]_{cyto}$. Over the past 15 years, many studies have shown that most of the activator calcium (up to 95% in species with fast heart rates, see Bers, 1991 for review) comes from intracellular stores in the sarcoplasmic reticulum (SR). Most studies have shown that this calcium is released by a process of calcium-induced calcium release (CICR; Endo, Tanaka & Ogawa, 1970; Ford & Podolsky, 1970; Fabiato, 1985) via calcium release channels, commonly referred to as 'ryanodine receptors' (RyRs). Release by CICR gives rise to a *paradox of control*, because the released calcium would be expected to trigger further release, leading to a regenerative, nearly all-or-none event. Yet many studies have shown that the rate and duration of SR calcium release are tightly controlled by the trigger calcium that enters the cell via voltage-controlled calcium channels. The need to resolve this paradox has led to the increasing popularity of 'local control' models of excitation–contraction coupling, in which the trigger for calcium release is the local calcium microdomain generated by influx through sarcolemmal calcium channels, and most of the gradation of release is due to statistical recruitment of localized release events. Using the terminology of Stern (1992), local control models can be roughly divided into 'calcium synapse' models, in which the elementary release event is the opening of a single release channel, locally

* To whom correspondence should be addressed.

controlled by a single triggering microdomain, and 'cluster bomb' models, in which the elementary event is a locally regenerative release by a group of release channels clustered together on an SR release terminal.

Shortly after local control models were proposed, Cheng, Lederer & Cannell (1993) discovered that localized, stochastic release events, dubbed 'calcium sparks', can be directly observed by confocal microscopy in single cardiac myocytes loaded with the fluorescent calcium probe fluo-3. Subsequent work (Cannell, Cheng & Lederer, 1995; López-López, Shacklock, Balke & Wier, 1995; Santana, Cheng, Gomez, Cannell & Lederer, 1996) has shown that calcium sparks are 'elementary events' of cardiac excitation–contraction coupling, in the sense that whole-cell calcium release can be plausibly reconstructed as a summation of these events. Nevertheless, the exact nature of sparks, and, in particular, whether they are due to single openings of release channels or to locally regenerative activation of clusters of such channels, remains controversial (Lipp & Niggli, 1996; see Cheng *et al.* 1996*b*; Ríos & Stern, 1997 for a review of the evidence). If the generation of an observable spark requires the recruitment of multiple release channels by local CICR, then spark occurrence should fail if the releasable calcium content of the SR is sufficiently reduced. If, on the other hand, sparks are due to single release channel openings, then reducing the unitary release flux by depleting the SR of calcium should have little effect on the rate of occurrence of spontaneous sparks, although there is some evidence that permeating calcium can modulate the gating of single release channels in lipid bilayers (Tripathy & Meissner, 1996; Lukyanenko, Györke & Györke, 1996). In either case, the amplitude of sparks is expected to depend on SR calcium content.

Testing the above predictions experimentally is not straightforward, for two reasons. First, amplitude and frequency statistics of sparks must be measured by confocal linescans. Sparks whose centres are not located on the scan line will appear smaller in amplitude than those which are centred on the line. This can lead to a major distortion of the apparent distribution of spark amplitudes, to the point of rendering the distribution non-modal even if the true calcium release events are entirely stereotyped (E. Ríos, M. Stern & H. Cheng, unpublished results). Second, sparks are small fluorescence increments which must be detected against a background of noise. This will lead to an underestimate of the number of low-amplitude sparks, and any intervention which reduces spark amplitude will reduce detectability, causing an apparent decrease in spark frequency.

To compensate for these problems, we developed an objective algorithm for the detection of sparks in confocal linescan images, and we recorded a large number of events to estimate the distribution of amplitudes at each level of SR calcium content. Allowing for reduced detectability of sparks below a normalized fluorescence ($\Delta F/F_0$) amplitude of 0·4, the results were consistent with the theoretical prediction that the distribution of apparent spark amplitudes (i.e. amplitudes as modified by offset from the scan line and/or sampling at the finite linescan repetition rate) would be monotonically decreasing. The apparent frequency of sparks decreased markedly when SR calcium content was reduced, while the mean spark amplitude fell only modestly. However, if the results were corrected for detection bias, it was found that the spark frequency is independent of SR load, while the amplitude is proportional to load.

METHODS

Adult ventricular myocyte preparation

Ventricular cardiac myocytes were isolated from adult Sprague–Dawley rats (age, 2–3 months; weight, 225–300 g) by collagenase digestion as described previously (Xiao, Valdivia, Bogdanov, Valdivia, Lakatta & Cheng, 1997). Briefly, following anaesthesia (sodium pentobarbitone, 100 mg kg^{-1} injected I.P.), the heart was removed from the chest and perfused retrogradely via the aorta using the Langendorff method and collagenase (Worthington type II, 1 mg ml^{-1}). Single cells were shaken loose from the heart following this perfusion procedure in Hepes buffer solution containing (mM): 137 NaCl; 5·4 KCl; 1·2 $MgCl_2$; 1·2 NaH_2PO_4; 1 $CaCl_2$; 10 glucose and 20 Hepes (pH 7·4). Myocytes were loaded with fluo-3 by 10 min incubation in buffer containing 10 μM fluo-3 AM (Molecular Probes), dissolved in DMSO, followed by a 15 min wash in fresh Hepes buffer.

Confocal microscopy of calcium sparks

Myocytes loaded with the indicator were studied on the stage of a Zeiss LSM-410 inverted confocal microscope in the linescan mode, with excitation by the 488 nm line of an argon laser. Cells were selected for study on the basis of (1) clear striation pattern, (2) contraction on electrical field stimulation by 5–15% of resting cell length, (3) a negative staircase on stimulation from rest, and (4) no spontaneous contractions during a 1 min observation period. Sparks were recorded in the confocal linescan imaging mode. Eight images were obtained at 5 s intervals, along eight evenly spaced parallel scan lines oriented along the long axis of the myocyte. Each image consisted of 512 lines scanned at intervals of 4·38 ms, 512 pixels per line spaced at 0·156 μm intervals. The microscope objective was a Zeiss Plan-Neofluar ×40 oil immersion lens (numerical aperture, 1·3). The optical resolution of the microscope was 0·5 μm in the horizontal plane and 1·0 μm in depth, as determined by imaging 0·09 μm fluorescent beads (Molecular Probes). All experiments were conducted at 23 °C.

SR depletion protocol

Releasable SR calcium content was determined by applying 500 ms puffs of 15 mM caffeine, delivered through a micropipette, using a Picospritzer (General Valve Co., NJ, USA). The pipette was located >200 μm downstream from the cell, and was placed about 50 μm upstream immediately before applying the puff. Each cell was studied by the following protocol. First, eight linescan images were taken in the resting cell; SR calcium load was then measured by a caffeine spritz. Next, the cell was field stimulated at 0·5 Hz, followed by a 2 min rest, in order to replete SR stores. After the cell was exposed to thapsigargin (25, 50, 100 or 150 nM) for 10 min, eight more linescan images were obtained. Remaining SR calcium was then measured by another caffeine spritz. Peak $[Ca^{2+}]_{cyto}$ was estimated from peak increase of normalized fluorescence, F/F_0, where F_0 denotes the resting fluorescence, using a pseudo-ratio

method (Cheng *et al.* 1993) and assuming a resting $[Ca^{2+}]_{cyto}$ of 120 nM and a dissociation constant (K_d) of fluo-3 for calcium 1·0 μM.

Detection and classification of sparks

In order objectively to identify and measure sparks, we developed an algorithm which selected sparks on the basis of their statistical deviation from background noise. The basic steps of the algorithm included: (1) estimating the mean (m_1) and variance (σ_1^2) (standard deviation (S.D.) $= \sqrt{\sigma^2}$) of the confocal image intensity after images had been subjected to a median filter using a 3×3 kernel and space–time smoothing (0·8 μm–17 ms or 6×4 window); (2) identifying candidate sparks by their excessive deviation from the mean value (the criterion for candidate sparks was pixel value of $m_1 + 2{\cdot}0\sqrt{(\sigma_1^2)}$ or greater); (3) recalculating background mean (m_2) and variance (σ_2^2) with the candidate sparks excised from the image; and (4) making a final selection of sparks by comparison with the background statistics. Two binary images were produced showing areas greater than $m_2 + 2{\cdot}0\sqrt{(\sigma_2^2)}$ (2-S.D. image) and areas greater than $m_2 + 3{\cdot}7\sqrt{(\sigma_2^2)}$ (3·7-S.D. image), respectively, and both images were subjected to a 5×5 median filter. A region counting program was then applied to count and to record the position of calcium sparks for future measurement: a spark event was registered if, and only if, a connected area in the 2-S.D. image was detected and the corresponding region in the 3·7-S.D. image has at least one non-zero pixel. Figure 1*A* shows a representative linescan image of a resting cardiac myocyte loaded with fluo-3. Three sparks identified by the automated algorithm are highlighted in the right panel, shown as separated islets in the corresponding 2-S.D. image. Figure 1*B* provides an example of a linescan record where the algorithm had detected a candidate small spark that would most likely not have been detected by eye. The amplitude of sparks so selected was reported as the peak value of F/F_0. The spatial diameter of sparks was indexed by the FWHM (full width at half-maximum) of the fluorescence profile of the spark. The spark duration, T_{50}, was measured at 50% level of the amplitude (Fig. 1*C*).

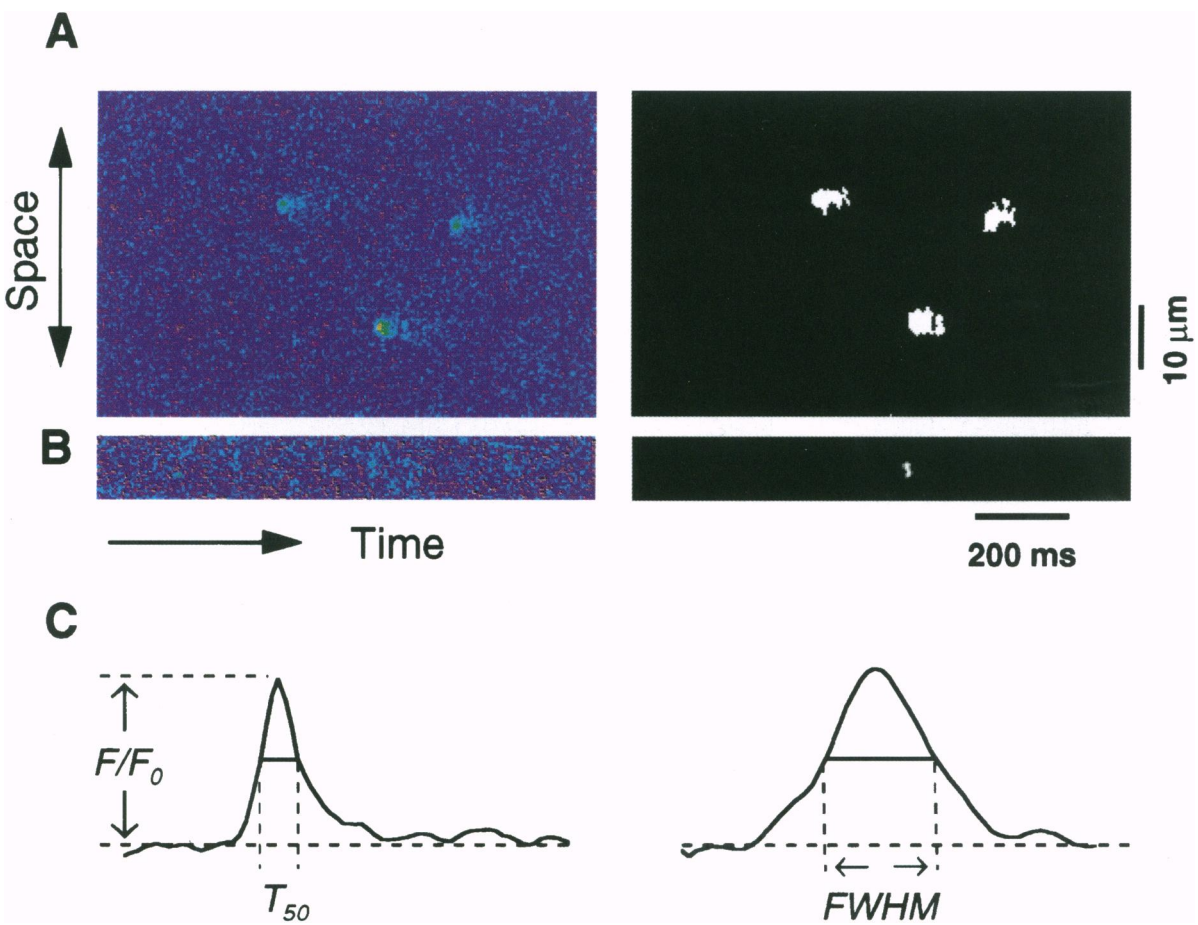

Figure 1. Detection and parametric measurements of calcium sparks

Left panel in *A*, a linescan image showing multiple spontaneous calcium sparks. Space and time are shown in the horizontal and vertical dimensions, respectively. Right panel in *A*, three spark events in the left panel identified and highlighted by the computer algorithm described in Methods. *B*, an example of linescan image where the algorithm has detected a candidate spark too weak to be identified by eye. *C*, representative plots of time course (left) and spatial profile at time of peak fluorescence (right) of a calcium spark. Parameters chosen to depict a spark event are (1) peak normalized fluorescence (F/F_0, where F_0 refers to baseline fluorescence prior to the spark), (2) dwell time above 50% level of the amplitude (T_{50}), and (3) spatial size indexed by the full width at half-maximum (FWHM).

RESULTS

Properties of sparks under control conditions

Under control conditions, sparks were detected by the automated algorithm at a rate of 1·50 ± 0·87 (mean ± S.D.), ranging from 0·35 to 4·26 events per second per 100 μm scan. Figure 2*A* shows a histogram of the amplitudes of 751 sparks in thirty-five myocytes, binned at intervals of 0·1 units of F/F_0. The distribution is highly skewed to the left, with a mean F/F_0 of 1·69 ± 0·38 (mean ± S.D.), a mode of 1·45, a median F/F_0 of 1·56, and minimum and maximum values of 1·22 and 3·36, respectively. This pattern is thus in contrast to previously reported stereotyped distributions when sparks were detected by eye (López-López *et al.* 1995; Lukyanenko *et al.* 1996; Cheng, Lederer, Lederer & Cannell,

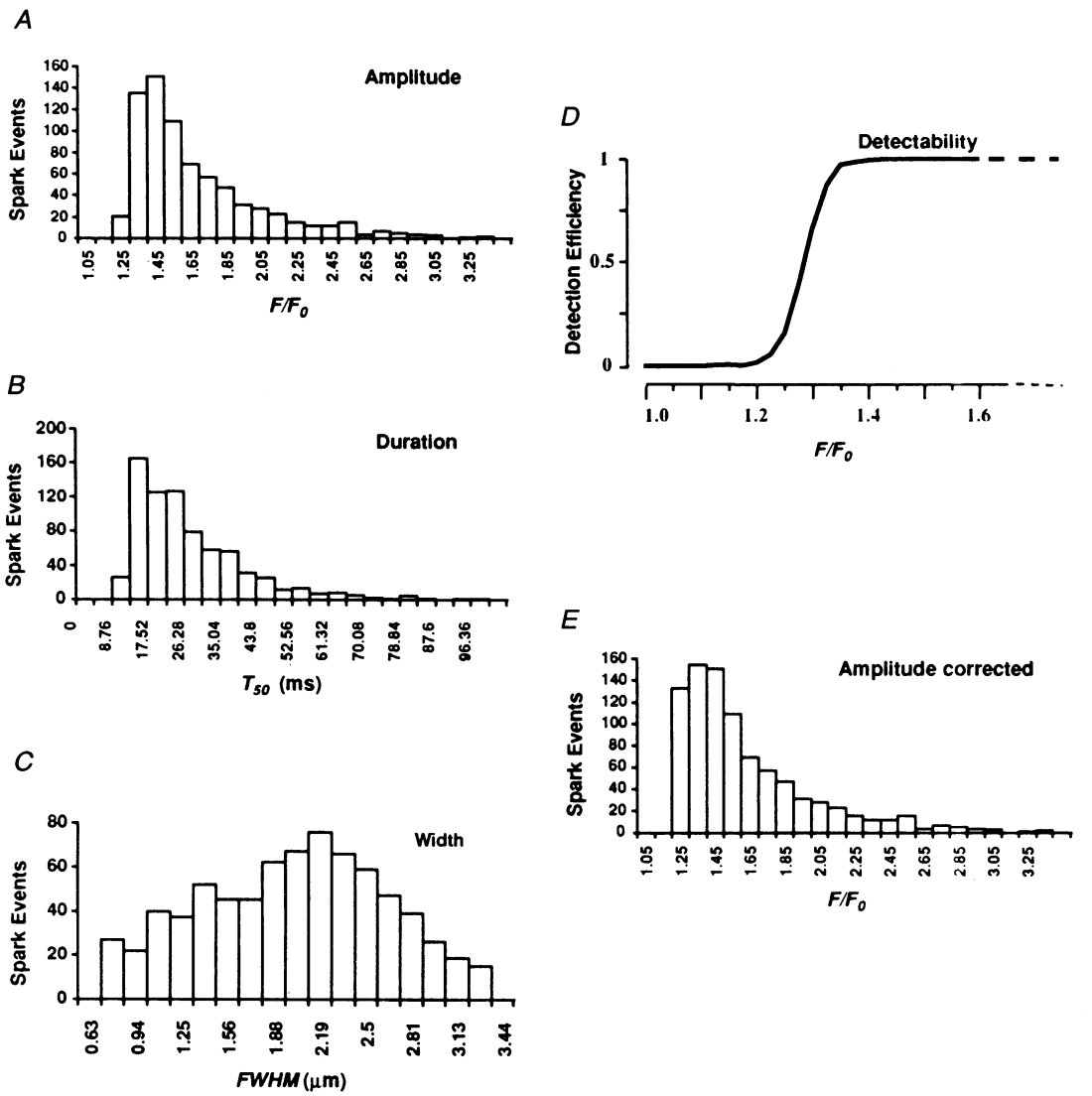

Figure 2. Properties of spontaneous calcium sparks under control conditions

Data were from 751 sparks in 35 cells. *A*, histogram of spark amplitudes indexed by F/F_0. The smallest spark detected had a peak of 1·22 and the largest a peak of 3·36. The optically recorded amplitude distribution is strongly skewed towards the low amplitudes, as expected from detection of release events located at a variable distance from the scan line (see text). *B*, duration histogram of calcium sparks. Data on T_{50} were binned every 4·38 ms, the linescan repetition rate. The extent of T_{50} is from 13·13 to 157·59 ms, with a mode of 17·52 ms. Nine events (1·2%) of duration greater than 100 ms are not shown. *C*, histogram of spark width, FWHM. The bin size is chosen as the pixel width of the linescan images (0·156 μm). The minimal and maximal spark breadths were 0·78 μm and 3·28 μm, respectively. *D*, detectability function for spark counting. An average spark was constructed from 35 spark events and this spark was then varied in intensity and embedded in random (Gaussian) noise at level comparable to that observed experimentally. A total of 5100 test images containing sparks of 1·0–1·6 were fed to the computer algorithm. *E*, amplitude distribution in *A* after correction for missing events.

1996*a*; Xiao *et al.* 1997), and to the well-known Gaussian distributions for electrophysiological recording of single ionic channel current. Figure 2*B* shows the distribution of control spark durations measured at the 50% level, with a mean lifetime of 38·8 ± 19·2 ms (mean ± S.D.), which is much longer than the mean open time of the cardiac ryanodine receptor in lipid bilayers (e.g. 5·4–22·3 ms with luminal pCa 4·8–2·0, Lukyanenko *et al.* 1996). An important contributor to the difference would be the time resolution of optical recording *in vivo* which is limited by the kinetics of the indicator and of local endogenous calcium buffers; the latter would act as calcium source after the cessation of local calcium release. As shown in Fig. 2*C*, the spatial diameter of the spark, FWHM, was broadly distributed over 0·78–3·28 μm, averaging 2·0 ± 0·63 μm (mean ± S.D.). There were surprisingly weak correlations among the three measured parameters: a positive correlation coefficient of 0·37 between amplitude and spatial extent, and a very weak, negative correlation (−0·18) between amplitude and duration. (In contrast, strong correlations would be expected if all of the variances in spark statistics were due entirely to variation in the position of a stereotyped event relative to the measurement line).

On the basis of theoretical considerations (see Discussion), we hypothesized that the skewed amplitude distribution represents an underlying monotonically decreasing distribution of apparent spark amplitudes (i.e. amplitudes as observed at the location of the confocal scan line), limited at the low-amplitude end by detectability. We measured the detection efficiency of our algorithm by testing the routine on an averaged spark which was scaled to different intensities and embedded in appropriate amounts of Gaussian noise. As the spark intensity varied, the detection efficiency rapidly decreased from ~1 at $F/F_0 = 1{\cdot}4$ to ~0 at $F/F_0 = 1{\cdot}2$. The criteria for spark detection were conservative as the detectability for spark amplitudes $\leqslant 1{\cdot}1$ was virtually nil (Fig. 2*D*); false detection was also extremely rare (1 event out of 48 blank 512 × 512 images containing noise only; data not shown). Figure 2*E* shows the corrected distribution of spark amplitudes which should have been observed if detectability were constant for all sparks of amplitude $\geqslant 1{\cdot}22$ (the smallest spark detected). If all sparks $\geqslant 1{\cdot}22$ were detected, there should be 832 instead of 751 events. That is, ~10% of sparks $\geqslant 1{\cdot}22$ were probably missed due to the inability to discern small sparks against background noise. (Note that there is still an apparent mode in this distribution, probably due to the fact that we had no information for spark amplitudes between 1·20 and 1·22 for the lowest bin.)

Effects of thapsigargin

Figure 3*A* shows the caffeine-releasable SR calcium after exposure to thapsigargin (25–150 nM), a specific SR calcium ATPase inhibitor (Kirby, Sagara, Gaa, Inesi, Lederer & Rogers, 1992; Janczewski & Lakatta, 1993). The SR load was estimated by the peak of the caffeine-induced calcium transient and expressed as a percentage of the calcium released by caffeine in the same cell prior to thapsigargin exposure. The releasable calcium after a 10 min exposure to thapsigargin decreased with increasing concentrations of thapsigargin up to a concentration of 150 nM. Higher concentrations produced no further depletion of the SR at 10 min. This is what would be expected if the SR calcium pump were completely blocked by 150 nM thapsigargin, and the rate of SR depletion in these resting cells was limited by the rate of leakage of calcium from the SR. Further depletion could be achieved by increasing the duration of thapsigargin exposure, but too few sparks could be detected under these conditions to obtain reliable statistics (data not shown). The responses of spark frequency and amplitude to thapsigargin are shown in panels *B* and *C*, respectively. of Fig. 3. Both spark rate and amplitude were reduced by thapsigargin in a dose-dependent manner. Thapsigargin at 150 nM, which depleted SR calcium to 35·9 ± 8·4% of control, reduced spark frequency to 29·7 ± 9·3% of control and spark amplitude only to 60 ± 5·0% of control. However, the resting fluorescence before and after thapsigargin exposure was not significantly altered (Fig. 3*D*), suggesting that cytosolic $[Ca^{2+}]$ was unchanged. Because fluo-3 is not a ratiometric probe, it was not possible to determine absolute levels of resting $[Ca^{2+}]_{cyto}$. Spark size showed a small but significant decrease with thapsigargin (Fig. 3*E*), while spark duration (Fig. 3*F*) showed minimal change except at the highest concentration of thapsigargin.

Correction of thapsigargin effects for sampling error

Since SR depletion reduces the amplitude of sparks, some sparks will then fall below the detection threshold, resulting in overestimation of mean spark amplitude and underestimation of spark number. We corrected the spark statistics after thapsigargin on the basis of the following two assumptions: (1) the observed amplitude distribution is the product of an underlying spark amplitude distribution and a fixed detection probability (Fig. 2*D*); (2) the effect of decreased SR loading would be to reduce the true spark amplitude, whether large or small, by a constant factor. In order to justify these assumptions, model distributions were generated from the control distribution by (a) correcting the control distribution by dividing by the detectability function for $F/F_0 \geqslant 1{\cdot}22$, as shown in Fig. 2*E*; (b) scaling the control amplitudes by an adjustable constant factor, *s*, and re-binning them at intervals of 0·1; (c) multiplying again by the detectability function. The scale factor *s* was adjusted to minimize the χ^2 statistic between the measured amplitude distribution after thapsigargin and the scaled control distribution. Figure 4*A* and *B* shows the measured amplitude distributions after application of 25 or 50 nM thapsigargin (columns), superimposed on the best-fitting scaled control distribution (○). There was no significant difference between the observed and scaled control distributions (χ^2 test; $P = 0{\cdot}339$, 125 sparks, for 25 nM

thapsigargin; $P = 0{\cdot}541$, 169 sparks, for 50 nM thapsigargin). Similar results were obtained at 100 nM ($P = 0{\cdot}24$, 43 sparks) and 150 nM thapsigargin ($P = 0{\cdot}338$, 64 sparks) (data not shown). This indicates that the observed distributions are compatible with assumptions (1) and (2) above, justifying their use to correct the observed frequency and amplitude statistics. Given the above results, we next generated the correction curves for spark frequency and amplitude as function of the scaling factor s (Fig. 4*C* and *D*). In each cell, the observed reduction in mean spark amplitude was used to estimate the factor s according to Fig. 4*D*, and subsequently, the correction coefficients for frequency (Fig. 4*C*) and for amplitude (the value of s itself).

Figure 4*E* plots relative spark frequency changes against remaining fraction of releasable SR calcium content. The continuous line shows the observed frequency changes. The dashed line shows frequency changes computed from the correction curves shown in Fig. 4*C* and *D*. These are estimates of the frequency changes which would have been observed if the effect of SR depletion were to reduce spark amplitude by a uniform scale factor, and all sparks whose amplitudes were $\geqslant 1{\cdot}22$ before this scaling were detected. Similarly, Fig. 4*F* plots mean spark amplitude *vs.* SR calcium, with the raw data (continuous line) above the estimated corrected amplitudes (dashed line). The correction of frequencies and amplitudes changes the interpretation altogether. The observed data, taken at face value, appear to show that the amplitude of sparks is reduced only modestly by SR depletion, and that this is accompanied by a marked reduction in the spark frequency. This is the pattern which would be expected if sparks were generated by a locally regenerative CICR process operating not far

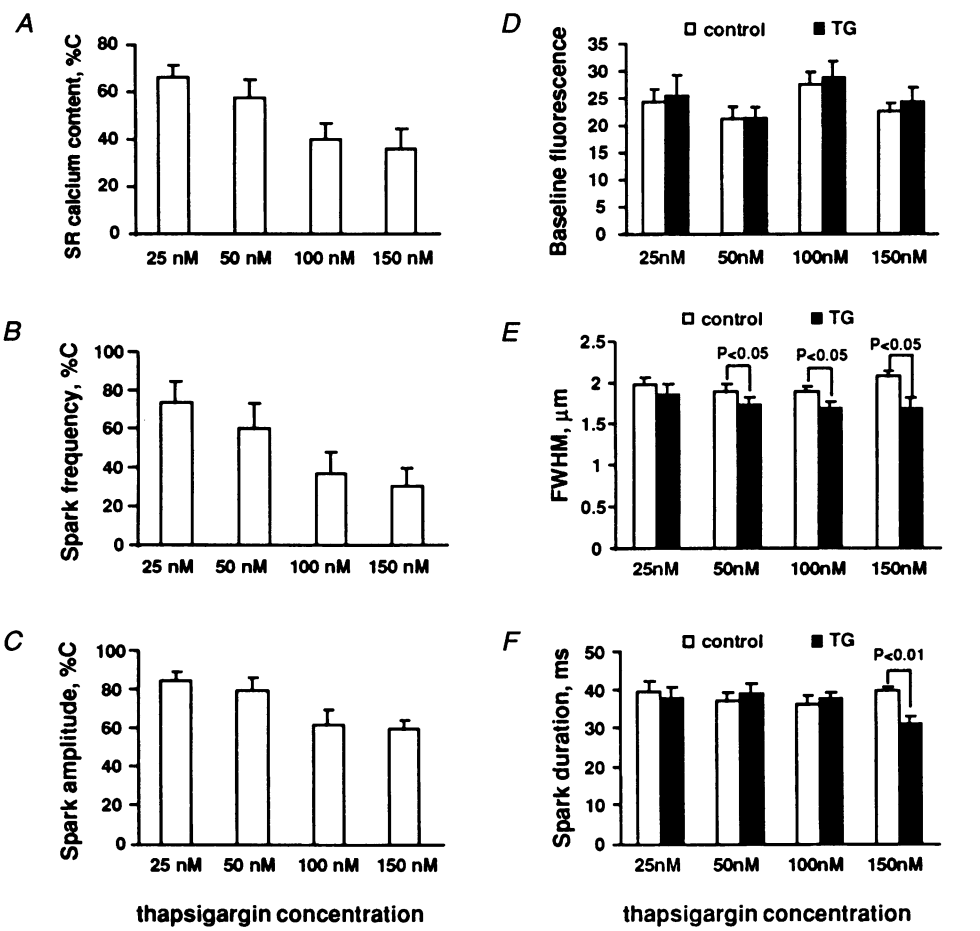

Figure 3. Effects of SR calcium loading status on elementary release events

A, partial depletion of caffeine-releasable SR calcium store by a 10 min exposure to 25, 50, 100, or 150 nM thapsigargin, an SR calcium ATPase inhibitor. SR filling status was determined by emptying the SR via rapid application of 15 mM caffeine. The resultant peak calcium transient, the index of the SR calcium load, was $1{\cdot}72 \pm 0{\cdot}46$ μM ($n = 28$, mean ± S.D.) under control conditions. Data were shown as the percentage of the control value (%C) in the same cell. *B*, decreases in calcium spark frequency induced by thapsigargin. Rate of spark occurrence prior to the drug was $1{\cdot}50 \pm 0{\cdot}87$ s^{-1} $(100\ \mu m)^{-1}$ ($n = 35$, mean ± S.D.). *C*, effect of thapsigargin on spark amplitude. *D–F*, baseline fluorescence intensity (*D*), spark width (*E*) and duration (*F*) under control conditions (open columns) and in the presence of thapsigargin (TG; filled columns). In all panels, $n = 5$–11 cells at each concentration.

above the threshold of regeneration. The estimated corrected frequencies and amplitudes show a frequency which is independent of SR load, and an amplitude which is proportional to load. This is the pattern which would be expected if sparks were due to single openings of single release channels whose unitary current was proportional to SR calcium content and whose on-gating rate was not affected by SR content or local release [Ca^{2+}].

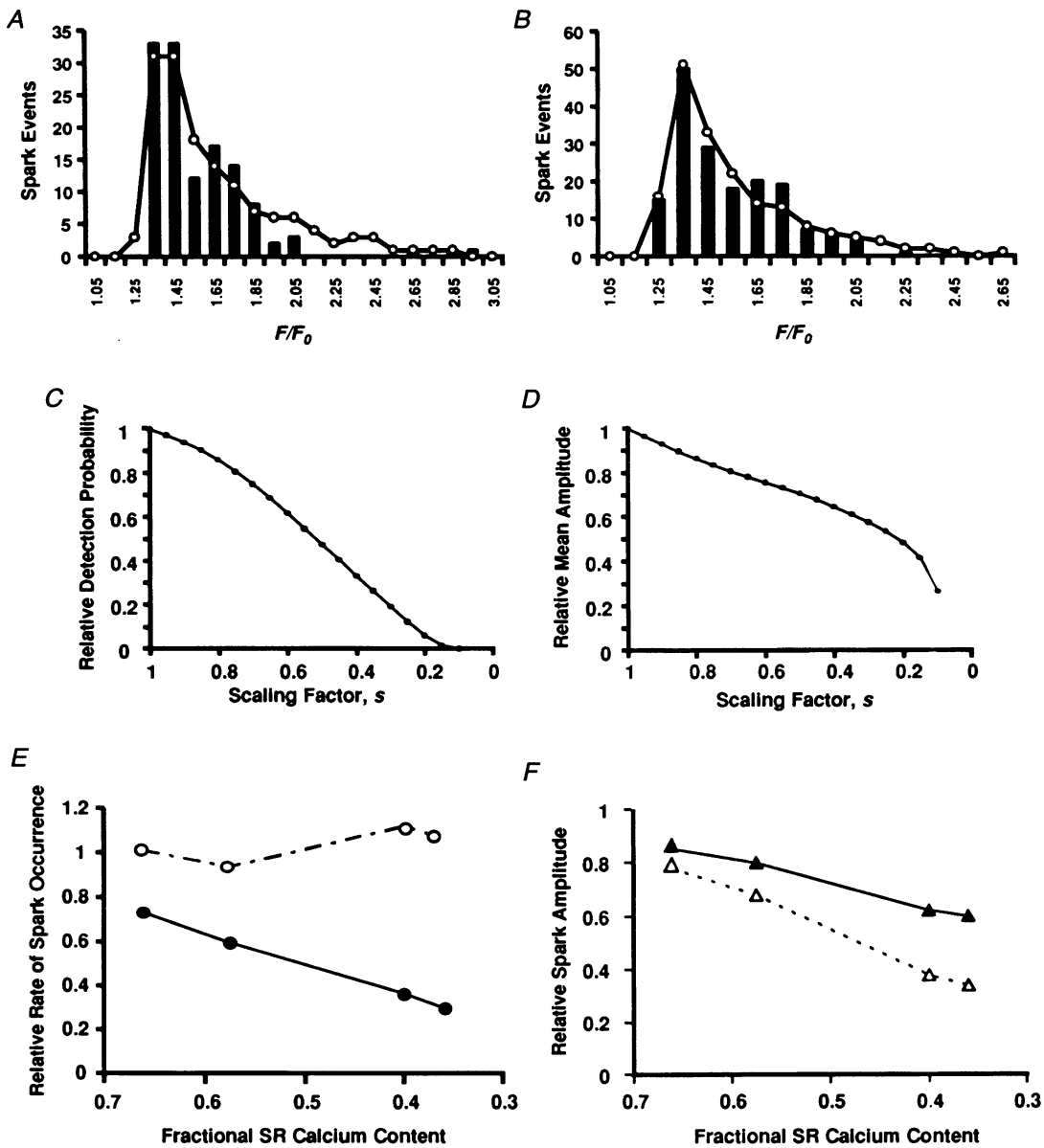

Figure 4. Correction of calcium spark amplitude and frequency for missing events due to detection efficiency

A and *B*, spark amplitude distributions in the presence of 25 nM (*A*) and 50 nM (*B*) thapsigargin. ○, observed data (filled columns) fitted by scaled control amplitude distributions (Fig. 2*E*) multiplied by the detection function (Fig. 2*D*). For results shown in *A* (125 sparks) and *B* (169 sparks), the goodness-of-fit values evaluated by χ^2 test were $P > 0{\cdot}339$ and $P > 0{\cdot}541$, respectively, consistent with the null hypothesis that the amplitude distribution after thapsigargin is the same as the scaled control distribution. *C* and *D*, predicted apparent reduction in spark frequency (*C*) and amplitude (*D*) as function of the scaling factor *s*. Curves were produced by scaling the amplitudes of control sparks (Fig. 2*E*) with the factor *s*, then calculating the number and mean amplitude of observable events assuming the detectability shown in Fig. 2*D*. *E*, relative rate of spark occurrence against changes in SR calcium load. ○, data before correction for detection efficiency; ●, data after correction for detection efficiency. (See text for correction methods.) *F*, mean spark amplitudes observed (▲) and after correction for missing events (△) as function of SR calcium content.

DISCUSSION

Calcium sparks: single-channel *vs.* multiple-channel hypothesis

Determining the nature of calcium sparks is one of the most critical issues for studies of excitation–contraction coupling. If sparks represent single openings of SR calcium release channels, then they offer a direct observation of the calcium release process at the smallest physiological length scale. If, on the other hand, sparks are due to regenerative gating of multiple release channels, then channel properties can only be inferred indirectly from spark data, in a model-dependent way. We attempted to distinguish between these two possibilities by studying the effect of reducing SR calcium stores. We reasoned that, if sparks are due to a calcium-mediated regenerative process, they might be abolished altogether by a modest reduction in the amount of released calcium which would reduce the positive feedback gain below the threshold for local regeneration. This did not occur: sparks were robustly observed, albeit at reduced frequency and amplitude, when SR calcium was depleted by nearly 2/3. Since the effect of SR depletion was quantitative rather than qualitative, definitive interpretation of the observed effects requires a correction for the major sampling bias introduced by confocal linescan imaging. After this correction (see below), the total number of sparks estimated was equal to the number of sparks (of amplitude greater than 1·22) present under control conditions, as if the *only* effect of SR depletion were to reduce the amplitude of all sparks by a constant factor (s). This result is what would be expected if sparks represent single openings of a channel whose opening rate is independent of the unitary calcium release flux, and is not modulated by $[Ca^{2+}]$ inside the SR. Further, when the same correction was used to estimate the mean amplitude of all sparks with amplitudes greater than $1 + 0{\cdot}22s$, it was found to be linearly correlated to releasable SR calcium content, which is a satisfying result, although it is not necessarily required that SR luminal $[Ca^{2+}]$ be linearly related to total releasable calcium, or that release channel unitary calcium flux be linearly proportional to luminal $[Ca^{2+}]$. The results of this study, as interpreted in the light of our simple statistical model of the spark detection process, are favourable to the single-channel hypothesis of spark generation. Even without statistical assumptions, our data show clearly that any model of the spark as due to multi-channel local regenerative CICR must be sufficiently robust to produce regenerative events even when only about 1/3 of the normal resting SR calcium load is present.

This may be understood more clearly with reference to the theoretically predicted behaviour of a cluster of CICR channels. Three regimes can be defined as a function of increasing unitary release flux (related to the releasable SR calcium content). In regime I the unitary release flux is small (relative to CICR sensitivity), so there is only a small probability that a spontaneous channel opening will recruit other channels in the cluster. In this regime, the frequency of events is independent of the permeating flux, and will depend on SR content only to the extent that the latter can directly influence release channel gating. The amplitude of fluorescence events, which is roughly proportional to release flux (G. Smith & H. Cheng, unpublished calculations), will be proportional to the unitary release flux. The *apparent* amplitude and frequency of *detected* events will be determined by the interaction of this proportional scaling with detectability, so that the estimated amplitude and frequency obtained by our correction procedure will give constant frequency and linear amplitude dependence, as we observed. In regime II the unitary flux is large enough to recruit additional CICR channels. For a sufficiently large cluster, there will be a narrow, threshold-like range of unitary flux over which the amplitude of events increases at a greater than linear rate from the amplitude characteristic of a single channel to that of the whole cluster. If, as suggested by Lipp & Niggli (1996), the single-channel events are too small to detect, then apparent frequency will rise rapidly in this regime, even after 'correction' by our method which assumes linear scaling of the amplitude distribution. Finally, in regime III, every opening of a channel triggers a regenerative activation of all the channels in the cluster. In this regime, the amplitude will again rise only linearly with unitary flux, since the number of activated channels is constant. The event statistics in regime III will therefore resemble those in regime I, except that the apparently 'elementary' event is actually a stereotyped cluster regeneration. The practical upper limit of regime III comes at the point where activation can spread to neighbouring clusters. In terms of these ideas, we can say that our data show that the range of SR loading between 36 and 100% of the normal resting value must lie entirely in regime I (single-channel openings) or entirely in regime III (robust cluster regenerations).

At first glance, our conclusions seem to be at odds with the observation by Parker, Zang & Wier (1996) that a majority of calcium sparks involves multiple sites hundreds of nanometres apart within the same Z-line zone. However, it is well-known that a continuum of behaviour of intracellular calcium dynamics can be observed under the 'same' experimental conditions (Wier, Cannell, Berlin, Marban & Lederer, 1987; Cheng *et al.* 1996*a*; Lukyanenko *et al.* 1996), presumably due to cellular inhomogeneity in calcium load. In rat ventricular myocytes, which exhibit spontaneous calcium waves and sparks, correlating observations with the frequency of waves and sparks seemed to us provide a practical way for a meaningful integration of results from different studies. Cells chosen in the present study were all quiescent during a 1 min observation period (see Methods) and had a rate of spontaneous sparks from 0·35 to $4{\cdot}26\ s^{-1}\ (100\ \mu m)^{-1}$ whereas spark rate in the study of Parker *et al.* (1996) appears to be much higher (31 and $48\ s^{-1}\ (100\ \mu m)^{-1}$, estimated from their Figs 1 and 3, respectively). Besides, our own data show rare radial or longitudinal regeneration of calcium sparks in rat and mouse ventricular myocytes (Cheng *et al.* 1996*b*) except in

cells showing higher frequency of calcium waves and calcium sparks (H. Cheng, unpublished observations). Therefore, the apparently conflicting observations could be reconciled, e.g. by a difference in SR loading conditions in these studies.

If our results are interpreted in favour of single-channel spark generation, then it becomes necessary to deal with a *paradox of independence*. How can single CICR channels gate independently when it is known that they are located in dense clusters? Simple diffusion calculations show that the local $[Ca^{2+}]$ in the vicinity of an open release channel will be large compared to the global value produced by photorelease in the experiments of Lipp & Niggli (1996) in which CICR was observed without discrete sparks. Local $[Ca^{2+}]$ at the cardiac diad junction is expected to be comparable to the levels required for steady-state activation of the cardiac RyRs in lipid bilayers, even in the presence of physiological $[Mg^{2+}]$ (Valdivia, Kaplan, Ellis-Davies & Lederer, 1995; Langer & Peskoff, 1996). Under these conditions it is difficult to imagine that RyRs act independently (regime I).

Optical sampling error and the correction algorithm

The confocal linescan samples fluorescence along a single line parallel to the long axis of the myocyte. While SR release channels are located almost exclusively at the plane of the Z-line of the sarcomere (Carl *et al.* 1995), there is no evidence that they have any preferred location within that plane. If sparks are located randomly within the plane of the Z-line, then the number of sparks located within a given perpendicular distance from the scan line will increase as the square of that distance. Calculations using simulated spark fluorescence profiles show that this would result in a distribution of apparent spark amplitudes which is monotonically decreasing, without a mode (E. Ríos, M. Stern & H. Cheng, unpublished results), and that it is nearly impossible to get a modal distribution using any plausible spark fluorescence profile (M. Stern & E. Ríos, unpublished results). Despite this, most published studies of calcium sparks selected by eye show a modal or multi-modal amplitude distribution.

To investigate this paradox, we developed an objective computer algorithm to identify and measure calcium sparks in confocal linescan images. This algorithm finds roughly twice as many sparks as are identified by eye (1·50 *versus* 0·73–0·85 s^{-1} $(100\ \mu m)^{-1}$ under control conditions; Cheng *et al.* 1996*a*,*b*; Lukyanenko *et al.* 1996), and they are predominantly small in amplitude, so that the resulting distributions both before and after thapsigargin are strongly skewed to the low-amplitude end. This distribution pattern is compatible with the theoretical prediction of a monotonically decreasing amplitude distribution, if we take the detection efficiency into account. Given the detectability function (Fig. 2*D*), it is possible to 'correct' the observed amplitude distribution to estimate the number of sparks which actually occurred with amplitudes greater than 1·22. In order to correct spark statistics during SR depletion, a further assumption is needed. It is necessary to extrapolate the number of sparks of amplitude less than 1·22, for which there is no information in the measured distribution from SR-depleted cells. In order to make this extrapolation in the least model-dependent way possible, we used the control amplitude distribution as an extrapolating function. This was done by assuming that the effect of SR depletion on spark amplitude is a uniform scaling of the amplitudes $\Delta F/F_0$ by a factor s between zero and one. The applicable factor was determined by a least-squares fit of the scaled control amplitude distribution to the measured amplitude distribution from SR-depleted cells. The goodness of fit was measured by the χ^2 test, which showed that the observed amplitude distributions from thapsigargin-treated cells were compatible with this scaling hypothesis. The scaled control distribution was then used to estimate the number of unobserved sparks which were present with amplitudes from $1 + 0{\cdot}22s$ to 1·22. As discussed above, this correction procedure significantly altered the scenario in interpreting data for SR calcium depletion. This methodology should be useful for future studies on physiological and pharmacological modulation of elementary release events.

Comparison with previous studies

Our finding that depletion of SR calcium reduced the apparent spark frequency is in agreement with the observation in rabbit ventricular myocytes in which both the SR calcium content and spark frequency are gradually decreased during rest after regular electrical stimulation (Satoh, Blatter & Bers, 1997). Previous *in vitro* studies using cell-free systems suggest that SR calcium may modulate RyRs (a) through direct or indirect (via calsequestrin) interaction from the luminal side (Fabiato, 1985; Ikemoto, Ronjat, Meszaros & Koshita, 1989; Kawasaki & Kasai, 1994; Györke, Lukyanenko & Györke, 1997), or (b) when released, binding to activation and inactivation sites of RyRs on the cytosolic side (Tripathy & Meissner, 1996). Since the resting $[Ca^{2+}]_{cyto}$ and the corrected rate of spark occurrence were unchanged when SR calcium was highly depleted, the present results indicate that SR intraluminal calcium content is not a major physiological modulator of ryanodine receptor gating *in vivo* under our experimental conditions (i.e. depletion of SR calcium). This underscores the importance of studying regulation of RyRs in intact cells and in the physiological context. Nevertheless, it should be pointed out that our data do not exclude the possibility that at elevated calcium load, luminal calcium could affect RyR gating (Fabiato, 1985; Stern, Capogrossi & Lakatta, 1988; Cheng *et al.* 1996*a*; Györke *et al.* 1997). In this regard, studies in cells challenged with 10 mM external Ca showed that a 30% increase in SR calcium is associated with a fourfold increase in the spark frequency (Cheng *et al.* 1996*a*; Lukyanenko *et al.* 1996). The increase in spark frequency is in part accounted for by increased $[Ca^{2+}]_{cyto}$, as we proposed previously (Cheng *et al.* 1996*a*). In the light of the present results, the spark frequency increase may also be

attributable to an enhanced detectability, since spark amplitudes are increased under calcium overload conditions.

Furthermore, the present data on elementary release events fit nicely with our previous findings at the whole-cell level that calcium transients elicited by L-type calcium current and the gain function of SR calcium release are linearly correlated with the caffeine-induced calcium transient (Janczewski & Lakatta, 1993; Janczewski, Spurgeon, Stern & Lakatta, 1995), as if the total number of release units recruited was unchanged but each had a proportionally reduced amount of released calcium.

The results of this study, when contrasted with those of other studies of spark statistics, in which sparks were identified by eye, show that the distributions of spark parameters are subject to strong observer selection bias, which can create an apparently normal distribution from events whose amplitudes are distributed monotonically. The criteria used in our spark identification algorithm were simple, and based largely on the amplitude of the event. It is possible that a more sophisticated method could discriminate nearby sparks from those farther from the scan line (for example, the rise time of nearby sparks ought to be faster); this would restore the ability to determine the mode (if any) of the underlying distribution of calcium release events. Model calculations show that this will be difficult with the present generation of fluorescent probes and detection hardware; more sophisticated methods need to be devised to determine the true nature of calcium sparks. In the meanwhile, it is necessary to be wary of the effects of selection bias in spark studies.

Bers, D. M. (1991). *Excitation–Contraction Coupling and Cardiac Contractile Force.* Kluwer Academic Publishers, The Netherlands.

Cannell, M. B., Cheng, H. & Lederer, W. J. (1995). The control of calcium release in heart muscle. *Science* **268**, 1045–1049.

Carl, S. L., Felix, K., Caswell, A. H., Brandt, N. R., Ball, W. J. Jr, Vaghy, P. L., Meissner, G. & Ferguson, D. G. (1995). Immunolocalization of sarcolemmal dihydropyridine receptor and sarcoplasmic reticular triadin and ryanodine receptor in rabbit ventricle and atrium. *Journal of Cell Biology* **129**, 673–682.

Cheng, H., Lederer, M. R., Lederer, W. J. & Cannell, M. B. (1996*a*). Calcium sparks and $[Ca^{2+}]_i$ waves in cardiac myocytes, *American Journal of Physiology* **270**, C148–159.

Cheng, H., Lederer, M. R., Xiao, R.-P., Gomez, A. M., Zhou, Y.-Y., Ziman, B., Spurgeon, H., Lakatta, E. G. & Lederer, W. J. (1996*b*). Excitation-contraction coupling in heart: New insights from Ca^{2+} sparks. *Cell Calcium* **20**, 129–140.

Cheng, H., Lederer, W. J. & Cannell, M. B. (1993). Calcium sparks: elementary events underlying excitation-contraction coupling in heart muscle. *Science* **262**, 740–744.

Endo M., Tanaka, M. & Ogawa, Y. (1970). Calcium induced release of calcium from the sarcoplasmic reticulum of skinned skeletal muscle fibres. *Nature* **228**, 34–36.

Fabiato, A. (1985). Time and calcium dependence of activation and inactivation of calcium-induced release of calcium from the sarcoplasmic reticulum of a skinned cardiac Purkinje cell. *Journal of General Physiology* **85**, 247–290.

Ford, L. E. & Podolsky, R. J. (1970). Regenerative calcium release within muscle cells. *Science* **167**, 58–59.

Györke, S., Lukyanenko, V. & Györke, I. (1997). Dual effects of tetracaine on spontaneous calcium release in rat ventricular myocytes. *Journal of Physiology* **500**, 297–309.

Ikemoto, N., Ronjat, M., Meszaros, L. G. & Koshita, M. (1989). Postulated role of calsequestrin in the regulation of calcium release from sarcoplasmic reticulum. *Biochemistry* **28**, 6764–6771.

Janczewski, A. M. & Lakatta, E. G. (1993). Thapsigargin inhibits Ca^{2+} uptake, and Ca^{2+} depletes sarcoplasmic reticulum in intact cardiac myocytes. *American Journal of Physiology* **265**, H517–522.

Janczewski, A. M., Spurgeon, H. A., Stern, M. D. & Lakatta, E. G. (1995). Effects of sarcoplasmic reticulum Ca^{2+} load on the gain function of Ca^{2+} release by Ca^{2+} current in cardiac cells. *American Journal of Physiology* **268**, H916–920.

Kawasakai, T. & Kasai, M. (1994). Regulation of calcium channel in sarcoplasmic reticulum by calsequestrin. *Biochemical and Biophysical Research Communications* **199**, 1120–1127.

Kirby, M. S., Sagara, Y., Gaa, S., Inesi, G., Lederer, W. J. & Rogers, T. B. (1992). Thapsigargin inhibits contraction and Ca^{2+} transient in cardiac cells by specific inhibition of the sarcoplasmic reticulum Ca^{2+} pump. *Journal of Biological Chemistry* **267**, 12545–12551.

Langer, G. A. & Peskoff, A. (1996). Calcium concentration and movement in the diadic cleft space of the cardiac ventricular cell. *Biophysical Journal* **70**, 1169–1182.

Lipp, P. & Niggli, E. (1996) Submicroscopic calcium signals as fundamental events of excitation- contraction coupling in guinea-pig cardiac myocytes. *Journal of Physiology* **492**, 31–38.

López-López, J. R., Shacklock, P. S., Balke, C. W. & Wier, W. G. (1995). Local calcium transients triggered by single L-type calcium channel currents in cardiac cells. *Science* **268**, 1042–1045.

Lukyanenko, V., Györke, I. & Györke, S. (1996). Regulation of calcium release by calcium inside the sarcoplasmic reticulum in ventricular myocytes. *Pflügers Archiv* **432**, 1047–1054.

Parker, I., Zang, W. J. & Wier, W. G. (1996). Ca^{2+} sparks involving multiple Ca^{2+} release sites along Z-lines in rat heart cells. *Journal of Physiology* **497**, 31–38.

Ríos, E. & Stern, M. D. (1997). Calcium in close quarters: microdomain feedback in excitation-contracion coupling and other cell biological phenomena. *Annual Review of Biophysical and Biomolecular Structure* **26**, 47–82.

Santana, L. F., Cheng, H., Gomez, A. M., Cannell, M. B. & Lederer, W. J. (1996). Relationship between the sarcolemmal calcium current and calcium sparks and local control of cardiac excitation-contraction coupling. *Circulation Research* **78**, 166–171.

Satoh, H., Blatter, L. A. & Bers, D. M. (1997). Effects of $[Ca^{2+}]_i$, SR Ca^{2+} load, and rest on Ca^{2+} spark frequency in ventricular myocytes. *American Journal of Physiology* **272**, H657–668.

Stern, M. D. (1992). Theory of excitation-contraction coupling in cardiac muscle. *Biophysical Journal* **63**, 497–517.

Stern, M. D., Capogrossi, M. C. & Lakatta, E. G. (1988). Spontaneous calcium release from the sarcoplasmic reticulum in myocardial cells: mechanisms and consequences. *Cell Calcium* **9**, 247–256.

TRIPATHY, A. & MEISSNER, G. (1996). Sarcoplasmic reticulum lumenal Ca^{2+} has access to cytosolic activation and inactivation sites of skeletal muscle Ca^{2+} release channel. *Biophysical Journal* **70**, 2600–2615

WIER, W. G., CANNELL, M. B., BERLIN, J. R., MARBAN, E. & LEDERER, W. J. (1987). Cellular and subcellular heterogeneity of $[Ca^{2+}]_i$ in single heart cells revealed by fura-2. *Science* **235**, 325–328.

VALDIVIA, H. H., KAPLAN, J. H., ELLIS-DAVIES, G. C. R. & LEDERER, W. J. (1995). Rapid adaptation of cardiac ryanodine receptors: Modulation by Mg^{2+} and phosphorylation. *Science* **267**, 1997–2000.

XIAO, R.-P., VALDIVIA, H. H., BOGDANOV, K., VALDIVIA, C., LAKATTA, E. G. & CHENG, H. (1997). The immunophilin FK506 binding protein (FKBP) modulates Ca^{2+} release channel closure in rat heart. *Journal of Physiology* **500**, 331–342.

Acknowledgements

We thank Dr Harold A. Spurgeon and Bruce Ziman for their excellent technical support, Dr Eduardo Ríos for allowing us to use his unpublished results, and Dr Rui-Ping Xiao for critical comments on the manuscript. This work was supported by a NIH intramural research program.

Authors' email addresses

H. Cheng: hcheng@umabnet.ab.umd.edu

M. Stern: mstern@welchlink.welch.jhu.edu

Received 10 June 1997; accepted 11 September 1997.